Malaysian Journal of Catalysis
http://mjcat.utm.my/
MJCat

Catalytic reduction of methyl blue using biosynthesized gold nanoparticles

Nik Mariam-Jamilah Nik Lukmanulhakin, Mustaffa Shamsuddin*
Department of Chemistry, Faculty of Science, Universiti Teknologi Malaysia, 81310 Johor Bahru, Malaysia
Corresponding author email: mustaffa@kimia.fs.utm.my

Article history :
Received 1 May 2017
Accepted 20 July 2017

GRAPHICAL ABSTRACT

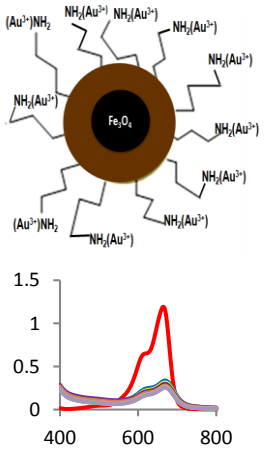

ABSTRACT

Gold nanoparticles (AuNPs) have attracted wide attention due to their significant applications in catalysis and environmental remediation. In particular, their high surface area to volume ratio contributes to their higher reactivity and made them a powerful tool for removal of contaminant in aqueous system. Green synthesis of AuNPs utilizing plant extract has been suggested as possible eco-friendly alternatives to chemical and physical methods. Due to their higher reactivity, AuNPs have tendency to agglomerate resulting in large particle size. Ligand assisted method employing functionalize ligands will covalently anchor the AuNPs onto the solid support thus controlling the AuNPs particle size and preventing agglomeration. In this research, a (3-aminopropyl)triethoxysilane (APTES)-functionalized silica-coated magnetite biosynthesized AuNPs was synthesized using *Cosmos caudatus* aqueous leaf extract as the reducing agent. The magnetic biosynthesized AuNPs were characterized by using FTIR, XRD and AAS analyses. FTIR spectroscopy confirmed that the biomolecules present in the *Cosmos Caudatus* leaf extract act both as reducing and capping agents. The XRD diffractogram showed that the crystalline AuNPs have been immobilized on the APTES-functionalized silica-coated magnetite. The data obtained from AAS analysis indicated that the amount of Au metal present was 5.5 wt%. The reactivity of the magnetic biosynthesized AuNPs was tested in the decolourization of methyl blue in aqueous solution. The concentration of the dye was monitored using UV- Vis Spectrophotometry. The reduction of methyl blue obeyed a pseudo first order reaction with the highest rate constant of 1.74×10^{-2} min^{-1}. The rate constant increases with the increase amount of catalyst. 83% decolourization of methyl blue was achieved suggesting that the catalyst is effective in removing methyl blue.

Keywords: Gold nanoparticles; (3-aminopropyl)triethoxysilane (APTES); biosynthesis; Cosmos Caudatus; reduction; methyl blue

| eISSN 0128-2581 |

1. INTRODUCTION

For the past few years, noble metals nanoparticles have received considerable attention owing to their unique properties which are promising in diverse fields with a variety of technological applications [1]. Due to the high surface area over volume ratio, metal nanoparticles exhibit special characteristics as compared to the bulk material. In particular, gold nanoparticles (AuNPs) showed excellent catalytic properties [2]. The inherent physical and chemical properties of AuNPs lead to their indispensable applications which can simply be tuned by tailoring the size and shape of nanoparticles. The particle size- and shape-controlling processes in synthesizing metal nanoparticles play an important role in manufacturing advanced materials on a large scale and therefore, well-controlled synthesis of nanoparticles is necessary to unambiguously correlate the structural properties of them with their catalytic properties [3].

There are several methods to synthesise AuNPs [4]. The traditional method of synthesizing gold nanoparticles utilised the use of high amount of organic solvent and also hazardous reducing agent such as $LiAlH_4$. These chemicals are very toxic to the environment. As a result, there is a growing demand to develop feasible, cost-effective, and environmentally safe procedures and conditions that favour the formation of shape-controlled metal nanoparticles. In recent years, the biosynthetic methods employing plant extract is gaining attention due to its simplicity and environmental friendly [5]. This method is more clean, reliable, biocompatible and eco-friendly.

Although metal nanoparticles are catalytically active, one major drawback of these particles is their tendency to agglomerate. In order to prevent aggregation, various approaches are pursued to stabilize the metal nanoparticles. These stabilizers should not interfere with the catalysed reaction or block the surface of the catalyst. Homogenously distributed metal nanoparticles could be stabilized by steric approach through the use of ligands [6].

Catalyst regeneration has always been an issue in heterogenous catalysis. The catalyst should be easily removed from product after the reaction. Usually, catalyst separation was done through filtration or centrifugation [7]. However, these methods are not effective in which some catalyst loss could not be avoided. Distillation and crystallization were also carried out with the aid of heat

especially for high molecular weight mixture. This requires high temperature to separate the product from the reaction mixture and thus might cause decomposition of catalyst which cannot withstand high temperature.

In order to overcome these issues, magnetic separation has been proposed as a new separation method as it is highly efficient, rapid, biocompatibility and low toxicity [8]. Magnetic separation by using magnetite (Fe_3O_4) is preferable as compared to other magnetic materials such as maghemite (γ-Fe_2O_3) due to its stability under most reaction conditions such as temperature, pressure, solvents, reagents, substrates and products. Besides that, the synthesis of magnetite Fe_3O_4 is relatively simple as compared to the synthesis of other magnetic materials.

2. EXPERIMENTS

In this research, magnetite (Fe_3O_4) nanoparticles (MNPs) was synthesized by co-precipitation method of Fe^{3+} and Fe^{2+} ion which then acted as the main support for the catalyst [9]. Second, the surface of the magnetite nanoparticles was coated with a silica layer by sol-gel method [10] followed by functionalization with (3-aminopropyl)triethoxysilane (APTES). The formation of magnetite, silica coated magnetite and APTES-functionalised silica coated magnetite was confirmed by FTIR analysis. Titration method was used to determine the amount of surface amino groups on the APTES-functionalized silica coated magnetite. Immobilization of AuNPs on the APTES functionalized silica coated magnetite was carried out through the absorption-reduction procedures using *Cosmos Caudatus* aqueous leaf extract as the reducing agent. Catalytic study of the magnetic biosynthesized AuNPs for the decolourisation of methyl blue was performed at room temperature. The reaction was monitored by UV-Vis spectroscopy.

3. RESULTS AND DISCUSSION

3.1 Synthesis and characterization of (3-aminopropyl) triethoxysilane (APTES)-functionalized silica-coated magnetite.

APTES-functionalized silica coated magnetite was first prepared by the co precipitation method of Fe^{2+} and Fe^{3+} ions in basic solutions. This led to the formation of magnetite nanoparticles. To avoid agglomeration the magnetite was then coated with silica by sol-gel method. Since iron oxide has strong affinity towards silica, a stable silica shell on the Fe_3O_4 surface had formed. Next, the silica coated magnetite nanoparticles were then functionalized with (3-aminopropyl) triethoxysilane (APTES). This APTES-functionalized silica coated MNPs was then characterized by using FTIR analysis and also titration method to determine the amount of surface amino groups.

Fourier Transform Infrared (FTIR) analysis

Successful silica coating and APTES functionalization of silica coated magnetite can be inferred from FTIR spectroscopic analysis. Figure 4.1 shows the FTIR spectrum of magnetite, silica coated magnetite and also APTES-functionalised silica coated magnetite. In the FTIR spectrum of magnetite, the signal observed at 572 cm^{-1} is attributed to the Fe-O bond vibration. In addition, two bands observed at 1583 and 1394 cm^{-1}, which are due to the COO-Fe bond and strongly suggested the complexation between the carboxylate moiety of citrate groups and iron on the magnetite nanoparticles surface. Sharp band at 1111 cm^{-1} corresponded to Si-O-Si anti-symmetric stretching vibration, being indicative of the existence of a SiO_2 layer around the magnetite. Furthermore, hydrogen-bonded silanols can be seen absorbed at around 3200 cm^{-1}. The presence of peaks at 2900 and 2800 cm^{-1} showed the presence of aliphatic C-H stretching vibrations. All the mentioned results confirmed the formation of a silica layer around the magnetite (Fe_3O_4) nanoparticles and the successful APTES functionalization of this core-shell structure.

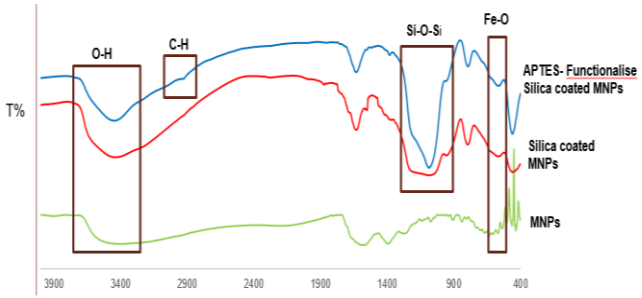

Fig. 1 FTIR spectrum of magnetite, silica coated magnetite and APTES-functionalised silica coated magnetite

Titration to determine the amount of amino surface group.

Experimentally, 0.02 g of APTES-functionalized silica coated magnetite was stirred with 100 mL of 0.0105M of hydrochloric acid for 2 hours. The mixture was then filtered and the filtrate was titrated with 1.0525 M of sodium hydroxide solution. It is found that 4.5 mL of NaOH is needed to neutralize the HCl. No of mole of NaOH used in the titration is equal to the number of mole of HCl unreacted with APTES-functionalized silica coated magnetite after 2 hours of stirring. Thus, it is found that there is 5.7473 x 10^{-5} mol of NH_2 in 0.02g of APTES-functionalised silica coated magnetite which equals to 2.8737 x 10^{-3} mmol g^{-1} of amino content.

3.2 Synthesis and characterization of gold nanoparticles

In this research, gold nanoparticles (AuNPs) were successfully synthesized by biosynthesis method which is through reduction of Au (III) by using leaf extract. The *Cosmos Caudatus* leaf extract acted as reducing and

surface capping agent. There are several phenolic compounds that have been reported to be an excellent antioxidant existed in the *Cosmos Caudatus* leaf extract. These compounds are proanthocyanidins, chlorogenic acids, quercetin and its derivatives. The presence of these biomolecules gave *Cosmos Caudatus* the great potential to act as reducing agent as well as capping agent for the reduction of metal ions to form metal nanoparticles and contributed to the stabilisation of the nanoparticles. AuNPs was characterized by using FTIR analysis, XRD analysis and AAS analysis.

Fourier Transform Infrared (FTIR) analysis

FT-IR spectroscopic analysis was carried out to describe the active functional groups which might be responsible for the reduction and capping of the nanoparticles. Figure 4.2 is the FTIR absorption spectra of *Cosmos Caudatus* leaf extract and Figure 4.3 is the FTIR spectra of supported gold nanoparticles (AuNPs). FTIR spectra of *Cosmos caudatus* showed several strong bands at 3218, 2933, 1590, 1393 and 1059 cm^{-1} which might be attributed to the presence of possible biomolecules that are responsible for the reduction and capping of AuNPs. A broad band at 3365 cm^{-1} revealed the O-H stretching vibrations, while peak at 2926 cm^{-1} is the asymmetric stretching of C-H groups. An adsorption band at 1059 cm^{-1} indicated the presence of C-OH stretching of secondary alcohols. FTIR spectra of supported gold nanoparticles (AuNPs) shows important peaks at 3400 cm^{-1} (O-H stretching vibrations), 2915 cm^{-1}(C-H vibration) and an absorption band 1732 cm^{-1} (carbonyl C=O). Most of the peaks observed in *Cosmos Caudatus* leaf extract can also be observed in the spectrum of the biosynthesized gold nanoparticles (AuNPs). Thus, it can be concluded that the biomolecules present in leaf extract are responsible to act as reducing and surface capping agent for the biosynthesised gold nanoparticles (AuNPs).

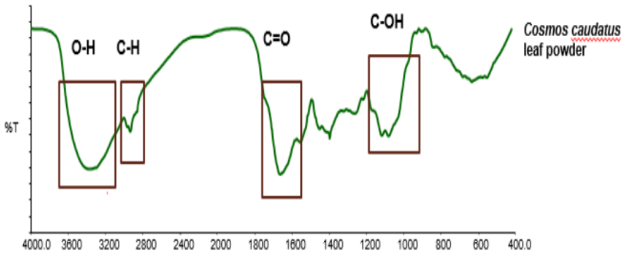

Fig. 2 FTIR spectrum of *Cosmos Caudatus* leaf extract

Powder X-ray Diffraction (XRD) Analysis

The crystalline nature of the biosynthesised AuNPs was confirmed from the X-Ray diffraction (XRD) analysis. Figure 4.4 shows the XRD pattern of the AuNPs obtained using aqueous leaf extract of *Cosmos caudatus*. The diffraction peaks observed at 2θ of 38.188°, 44.386°, 64.578° and 77.569° corresponded to the (111), (200), (220) and (311) facets of the face centered cubic (fcc) structure of metallic gold, respectively (JCPDS no. 04-0784. The XRD peak was also used to estimate the mean nanoparticle diameter by Scherrer's formula $D = 0.9\lambda/\beta \cos\theta$, where D is the average crystalline size, λ is the X-ray wavelength (1.542 Å), β is the angular linewidth of half-maximum intensity and θ is Bragg's angle in degree. The mean crystallite size calculated using this formula is about 19.8 nm.

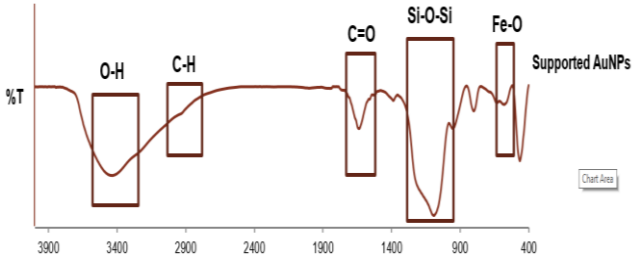

Fig. 3 FTIR spectra of supported gold nanoparticles (AuNPs)

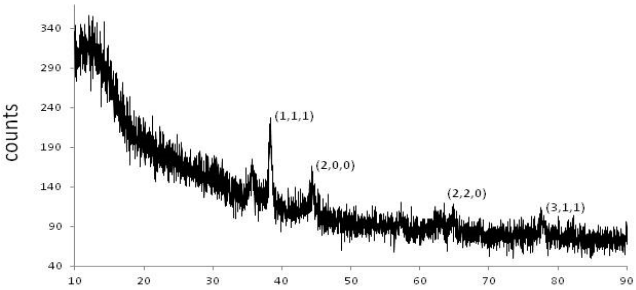

Fig. 4 XRD Diffraction patterns of biosynthesised AuNPs

AAS analysis

The amount of gold immobilized on the APTES-functionalized silica coated magnetite was determined by atomic absorption spectroscopy. The result obtained showed that there is 5.5 wt% in the gold content.

3.3 Catalytic study of biosynthesized gold nanoparticles (AuNPs) for the decolourization of methyl blue

One of the main application of nanomaterials is to catalyze reactions or activate chemical bonds that are otherwise not reactive. Catalytic applications of gold nanoparticles (AuNPs) have attracted considerable attention in recent years. In this study, the biosynthesized AuNPs have been tested in decolourization of methyl blue.

Uv-Vis Spectroscopy

In this catalytic study, the biosynthesized gold nanoparticles (AuNPs) was tested for the decolourization of methyl blue and recorded by using UV-Vis spectroscopy. This biosynthesized gold nanoparticles (AuNPs) were used

as catalyst in this reaction. Methyl blue have absorption in the visible spectrum and are concentration dependent.

Reaction mixture of methyl blue with only *Cosmos Caudatus* leaf extract and also methyl blue with only catalyst were kept as controls. Figure 4.5 and Figure 4.6 shows the UV-Vis spectra of these control experiments. The maximum absorbance of methyl blue that appeared at 664 nm underwent gradual decrease in both reaction mixtures. 63% decolourization of methyl was achieved in the presence of *Cosmos Caudatus* leaf extract while 56% decolourisation of methyl blue was achieved in the presence of 10 mg catalyst within 1 hour reaction. This shows that methyl blue undergo reduction process in both conditions. The decrease in the absorbance maximum is indicative of the ability of *Cosmos Caudatus* plant extract and catalyst to reduce methyl blue independently.

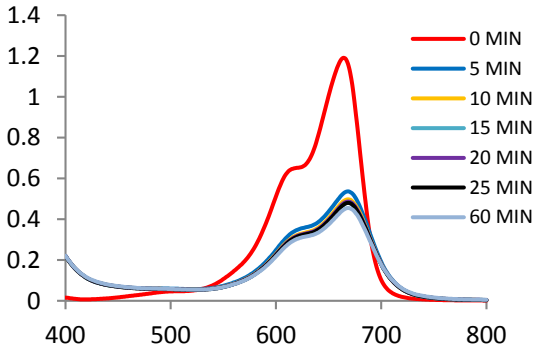

Fig. 5 Uv-Vis spectra of decolourisation of methyl blue in the presence of (3 mL) *Cosmos Caudatus* leaf extract.

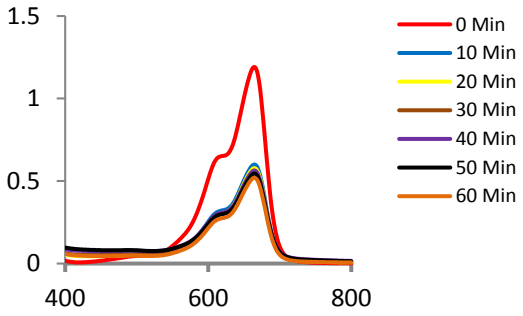

Fig. 6 Decolourisation of methyl blue in the presence of (10 mg) catalyst

Uv-Vis spectra for the decolourisation of methyl blue in the presence of *Cosmos Caudatus* leaf extract (3 mL) together with the catalyst (10 mg) was then carried out to observe the decolourization percentage of this reaction mixture within 1 hour reaction. From Figure 4.7, it is observed that the intensity of the maximum absorbance at 664 nm had decreased with a much higher reaction rate within 1 hour reaction as compared to the control experiments. 83% decolourization of methyl blue was achieved from this reaction mixture which is higher than percentage of decolourisation in both control experiments. Thus, this data confirmed that the biosynthesized gold nanoparticles (AuNPs) are catalytically active and able to catalyze the decolourization of methyl blue.

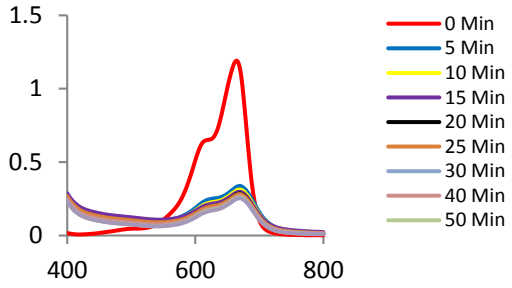

Fig. 7 Decolourisation of methyl blue in the presence of (3 mL) *Cosmos Caudatus* leaf extract and (10 mg) catalyst.

The amount of catalyst used was then varied in order to investigate the relationship between the amount of catalyst used and the rate of reaction. Based on the Uv-Vis spectra and the calculated reaction rate, it can be concluded that the higher the amount of catalyst, the higher the rate constant and thus, the higher the percentage of decolourization of methyl blue. Table 4.1 shows the rate constant for the decolourisation of methyl blue with 3 mL *Cosmos Caudatus* leaf extract and 5, 10 and 15 mg of catalyst. It was observed that 15 mg catalyst gives the highest rate constant which is 1.74×10^{-2} min^{-1} and 89% of decolourisation of methyl blue was achieved after 60 minutes operation.

Table 1: Rate constant for decolourisation of methyl blue

Amount of catalyst (mg)	Rate constant (Min^{-1})
5 mg	0.0047
10 mg	0.0146
15 mg	0.0174

4. CONCLUSION

In this research, the magnetite support was successfully synthesised and characterised. Silica layer was successfully coated on the surface of magnetite and confirmed by FTIR spectroscopy. Functionalisation of MNPs-Si was successfully done by (3-aminopropyl)triethoxysilane (APTES). This research also has demonstrated that *Cosmos Caudatus* plant extract is an excellent bioreductant and capping agent which provides an environmental friendly, cost effective and simple route for the synthesis of Au nanoparticles. This green synthesis route was generally a single step reaction and eliminates the use of additional chemical stabilizer or capping agent. The pholyphenolic compounds present in *Cosmos Caudatus* plant extract are believed to be responsible for the reduction of Au nanoparticles. The formation of Au nanoparticles was confirmed by the FTIR analysis. The conformation of biosynthesized AuNPs are amorphous in

nature was determined by using XRD analysis. The size of nanoparticles formed is 19.8 nm based on calculation by using Scherrer's formula. The obtained AuNPs was successfully utilized as catalyst for reduction of methyl blue. The catalytic ability of AuNPs was successfully confirmed by the decolourisation of methyl blue and the process is monitored by Uv-Vis spectroscopy. It is found that higher amount of catalyst will give higher rate constant.

ACKNOWLEDGEMENTS

The authors thank the Ministry of Higher Education Malaysia (MOHE) and Universiti Teknologi Malaysia (UTM) for their financial support through FRGS funding (Vote number 4F779).

REFERENCES

[1] Y.C. Yeh, B. Creran, V.M. Rotello, Nanoscale, 4 (2012), 1871.
[2] M. Stratakis, H. Garcia, Chem. Rev, 112 (2012), 4469.
[3] M. Grzelczak, J. Pérez-Juste, P. Mulvaney, L.M. Liz-Marzán. Chem. Soc. Rev, 37 (2008), 1783.
[4] A.K. Khan, R. Rashid, G. Murtaza, G., A. Zahra, Trop. J. Pharm. Res., 13 (2014), 1169.
[5] M.S. Akhtar, J. Panwar, Y.S. Yun, ACS Sustain. Chem. Eng., 1 (2013), 591.
[6] D. Astruc; F. Lu; J.R. Aranzaes, Angew. Chem. Int. Ed., 44 (2005), 7852.
[7] H. Yang, T. Zhou, W. Zhang, Angew. Chem., 125 (2013), 7603.
[8] A. Ali, M.Z. Hira-Zafar, I. Ul-Haq, A.R. Phull, J.S. Ali, A. Hussain, Nanotechnol Sci Appl, 9 (2016), 49.
[9] S. Saif, A. Tahir, Y. Chen, Nanomaterials, 6 (2016), 209.
[10] E. Ghasemi, E., M. Ghahari, Int. J. Nanosci. Nanotechnol, 11 (2015), 133.